Adsorption 3, 259–267, 2000

The Adsorption of $CHClF_2$ on NaY5.6 Zeolite

MITSUHIRO YOSHIKAWA
Department of Physics, Saitama University, Urawa 338-8570, Japan

TOSHIHISA YOSHIDA*
Department of Science Education, Saitama University, Urawa 338-8570, Japan
tyoshida@post.saitama-u.ac.jp

MITSUMASA ISHIWATA
Department of Physics, Saitama University, Urawa 338-8570, Japan

TOSHIO HASEGAWA
Department of Chemistry, Saitama University, Urawa 338-8570, Japan

SENTARO OZAWA
Department of Materials-process Engineering and Applied Chemistry for Environments, Akita University, Akita 010-8502, Japan

Received January 20, 2000; Revised May 15, 2000; Accepted May 26, 2000

Abstract. The adsorption of $CHClF_2$ on NaY5.6 zeolite has been studied by measuring the H and F NMR of the adsorbed $CHClF_2$, focusing in particular on the measurements of the chemical shift and longitudinal relaxation time, as well as the adsorption isotherm measurements. It is possible to determine the coordination structure of the $CHClF_2$ adsorbed on NaY5.6 zeolite by measuring the adsorption amount dependence of the chemical shift. In addition, the motional activity of the adsorbed molecules in the super cage of the zeolite is discussed on the basis of observed longitudinal relaxation times for various adsorption amounts.

Keywords: adsorption, zeolite, chlorodifluoromethane, adsorption structure, H and F NMR, chemicalshift, relaxation time, adsorbate mobility

1. Introduction

The catalytic properties of synthetic zeolites stem from their capacity to adsorb a variety of molecular species into the interconnecting cavities and channels within the framework structure where the cations are located. To understand the catalytic behavior of zeolites requires knowledge not only of the distribution of the cations, but also of the interaction between the cations and the adsorbed molecules and amongst the adsorbed molecules themselves. Even this is not sufficient, however; it is only necessary to know the location of the adsorbed molecules and their mobility in the cage. Although typical adsorbates such as nonpolar methane and aromatic benzene have been widely investigated both by means of theoretical calculation (Van Dun and

*Author to whom correspondence should be addressed.

Mortier, 1988; June et al., 1990; Yashonath et al., 1991) and by means of practical experiment (O'Mally, 1990; Liu et al., 1992; Pearson et al., 1992; Talu et al., 1993), there is at present very little study on polar hydrochlorofluorocarbon. The present paper is concerned with chlorodifluoromethane ($CHClF_2$) adsorbed on NaY5.6 zeolite ($Si_2/Al = 5.6$).

Recently, Wylie et al. (1995) observed Raman spectra of this $CHClF_2$ molecule adsorbed on NaY zeolite. They suggested that no direct interaction occurred between the C-H bond and the oxide surface, and that physical adsorption was dominant in this system, that is, where the quasi-liquid state and the surface phase coexisted in their high loading condition. We ourselves have already reported similar findings relating to the adsorption behavior of Xe on NaY zeolite observed by ^{129}Xe NMR, and we have shown that there are two distinct kinds of Xe adsorbed species, one trapped on the internal surface of the supercage and the other freely mobile within the framework structure (Yoshida et al., 1988, 1989).

The rather spherical $CHClF_2$ molecule has a relatively small radius (0.43–0.56 nm)(Beeson et al., 1962) as well as a large dipole moment ($\mu = 1.46$ debye), and contains two kinds of halogen atoms. Further information on this $CHClF_2$ molecule is needed in order to understand how to protect the ozone layer. The $CHClF_2$ molecule also contains the magnetic nuclei ^{1}H, ^{19}F and ^{13}C. Since the ^{1}H and ^{19}F have high NMR sensitivities, we used these nuclei as probes to learn more about the adsorptive behavior of this molecule. Recently, one of us has analyzed FTIR data of the $CHClF_2$ molecule adsorbed on ZSM-5 zeolite and proposed an adsorptive structure model of the $CHClF_2$ adsorbate (Katoh et al., 1997). In this paper, we have presented direct experimental evidence for this model based on the NMR data, and we discussed the changes in adsorption behavior as the adsorption amount varied; this last information was obtained by use of NMR spectroscopy and adsorption isotherm measurements.

2. Experimental

The adsorbent we used was commercial synthetic NaY5.6 zeolite (Union Showa Co., ltd., Japan), and the adsorbate was commercial $CHClF_2$ gas (Mitsui Du Pont fluoro chemical Co., ltd., Japan, 99.9%up). The zeolite was pretreated by being slowly heated to 400°C and kept at that temperature for 12 h under a vacuum of 10^{-5} Torr (1 Torr = 1.333 hPa). After being distilled three times to purify it, the $CHClF_2$ gas was adsorbed on the zeolite at a constant temperature. The adsorption amounts of the $CHClF_2$ gas were measured at 0, 10, and 20°C on a volumetric apparatus.

By using adsorption isotherms, sample tubes were sealed for the NMR measurement; these contained various adsorption amounts of the $CHClF_2$ molecule, under the corresponding equilibrium pressure, at 20°C. These samples did not contain any substance for the NMR field lock.

In order to obtain a highly stable magnetic field in which to measure the chemical shift, we used superconductive NMR spectrometers of AC 200 (Bruker Co., ltd., Japan) for the H nucleus and of AM 400 (Burker Co., ltd., Japan) for the ^{19}F nucleus. The H and ^{19}F resonance frequencies of the $CHClF_2$ molecule were determined with respect to those of TMS and $CFCl_3$, respectively. The standard substances in each separate tube were observed both before and after every measurement of the adsorbed sample, in order to check the chemical shift data. The chemical shift measurements were taken at the regulated room temperature of 20°C. Depending on the adsorption amount, signal accumulations were performed with 80–160 scans for H at 200 MHz and 25–96 scans for ^{19}F at 376 MHz.

For the longitudinal relaxation measurements of H and F nuclei, an FX90Q spectrometer (JEOL ltd., Japan) was used under the deuteron external lock. For the various adsorption amounts of the samples, longitudinal relaxation times were measured by the inversion recovery method (Martin et al., 1980a) at the regulated room temperature of 20°C. Signal accumulations were performed with 32–800 scans for H at 89.5 MHz and 16–400 scans for ^{19}F at 84.2 MHz, depending on the adsorption amount. Relaxation times were determined by use of the absorption peak areas. For some adsorption amounts, we also measured the relationship between temperature and relaxation times for H and F nuclei; the temperature range was from -25 to $+25$°C. The sample temperature was regulated nominally within 0.3°C using a conventional gas flow system.

3. Results and Discussion

3.1. Adsorption Isotherms and Adsorption Heat of the $CHClF_2$ Molecule

Figure 1 shows adsorption isotherms obtained from the adsorption amounts which were determined by the volumetric measurements at 0 and 20°C. The solid

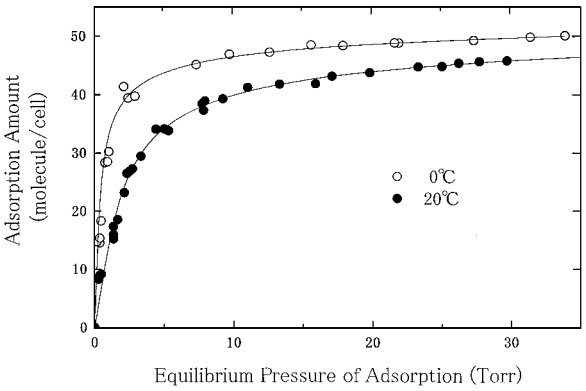

Figure 1. Adsorption isotherms of the $CHClF_2$ molecule on NaY5.6 zeolite at 0 and 20°C. The curves are the result obtained from the least square fit of the adsorption parameters to the experimental data.

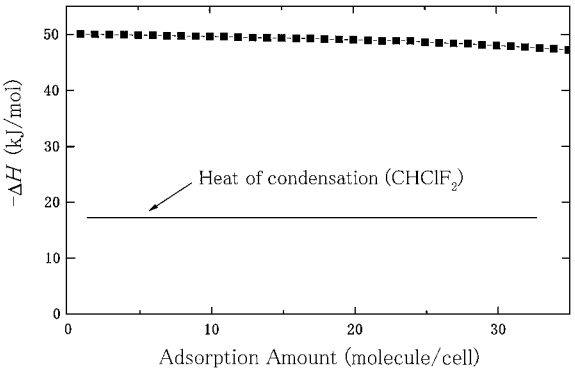

Figure 2. Adsorption amount dependence of the isosteric differential heat of adsorption ($-\Delta H$) for the $CHClF_2$ molecule on NaY5.6 zeolite. The horizontal straight line shows the heat of condensation.

lines in this figure are the result of curve-fitting simulations based on Hill's equation (Hill, 1946, 1947). These will be discussed in detail in Section 4. The ordinate of Fig. 1 is the number of the adsorbed $CHClF_2$ molecules per unit cell of NaY5.6 zeolite; one unit cell is $Na_{50}(AlO_2)_{50}(SiO_2)_{142}$ as a dried zeolite. In the adsorption isotherms, the number of the adsorbed molecules increases linearly with an equilibrium pressure up to approximately 30 molecules per unit cell and then begins to saturate. This number of the $CHClF_2$ molecules corresponds to the number of Na atoms per unit cell which is widely accepted to exist on the wall surface in the super cage of NaY5.6 zeolite (Sherry, 1968; Mortier et al., 1984). From the correlation of the two numbers in the lower range of adsorption, it should be noted that the Na atom on the surface is an adsorption site for the $CHClF_2$ molecule.

The isosteric differential heats of adsorption obtained from the adsorption isotherms are plotted in Fig. 2; these are charted for various adsorption amounts, together with the condensation heat of the $CHClF_2$ molecule. Thus we obtain approximately 50 kJ/mol of the adsorption heat ($-\Delta H$) for the $CHClF_2$ on NaY5.6 zeolite. Since this heat is considerably stronger than the condensation heat of 18 kJ/mol (Katoh et al., 1997), the adsorption in the present case is in a regime of strong physical adsorption. The gradual decrease in the adsorption heat together with the increasing adsorption amount reflects an increase in the mobility of the adsorption molecule in the zeolite cage, an increase which will be discussed in the following sections.

3.2. H and F NMR Spectra of the Adsorbed Molecule and Their Chemical Shifts

The NMR spectra of the H and F nuclei in the $CHClF_2$ molecule adsorbed on NaY5.6 zeolite were measured for adsorption amounts over the range of approximately 7 to 50 molecules per unit cell. Every measured H and F spectrum was a single broad band with a nearly Lorentzian line shape and the full half widths of 200 to 250 Hz. As compared with the sharp H and F spectra of a neat $CHClF_2$ liquid having line widths of 20–30 Hz and multiplet structures, due to the spin-spin coupling between H and F nuclei at approximately 60 Hz, the broad bands show a low mobility of the adsorbed molecules and the resulting strong magnetic interactions of the nuclear spins. In the line width of the NMR spectra we also found a weak dependence on the adsorption amount. For example, the full half width of the H spectra was approximately 240 Hz for 10–30 molecules per unit cell, while it was 210 Hz for 40–50 molecules per unit cell. This decrease in Hz, together with the increase in adsorption amount, reflects an increase in the mobility of the adsorbed molecules.

The dependences of the chemical shift on the adsorption amount are shown in Figs. 3 and 4 for H and F nuclei, respectively. The H spectrum for the smallest adsorption amount in our experiment appears at the lowest magnetic field. It corresponds to the finest screening and therefore to the largest chemical shift with respect to TMS (Pople et al., 1959). On the other hand, the F spectrum for the smallest adsorption amount shows the coarsest screening and therefore the smallest chemical shift with respect to $CFCl_3$. In these

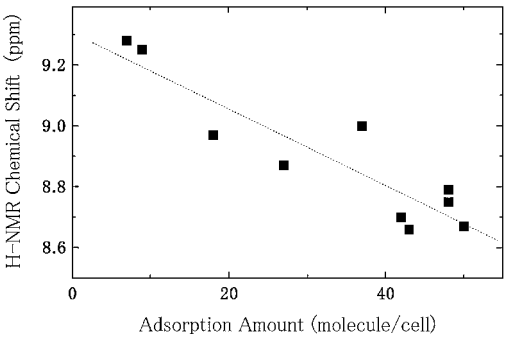

Figure 3. Adsorption amount dependence of the H NMR chemical shift of the $CHClF_2$ molecule adsorbed on NaY5.6 zeolite at 20°C. The chemical shift is referred to TMS.

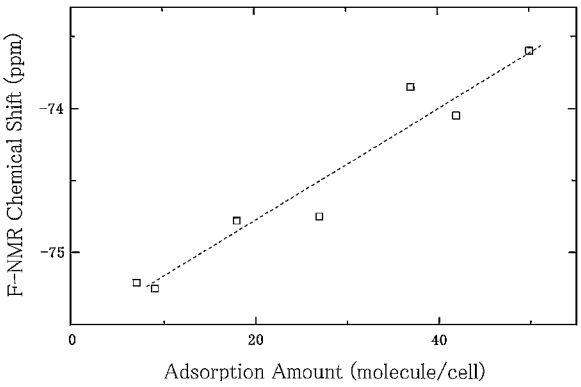

Figure 4. Adsorption amount dependence of the F NMR chemical shift of the $CHClF_2$ molecule adsorbed on NaY5.6 zeolite at 20°C. The chemical shift is referred to $CFCl_3$.

figures we can see gradual and nearly linear changes in the chemical shifts with the increase in the adsorption amount. This is an upfield shift for the H line and a downfield shift for the F, which corresponds to the more effective screening of the H nuclei and the less effective of the F nuclei, respectively. These chemical shift changes indicate that electrons in the $CHClF_2$ molecule gather exclusively to the side of the F atoms in the lowest range of adsorption amounts, and that the electrons will instead be repelled from F atoms as the adsorption amount increases.

The cage surface of NaY5.6 zeolite consists mainly of negatively charged oxygen atoms and positively charged, charge-compensating Na atoms. Since the polar $CHClF_2$ molecule has excess negative charges around the halogen atoms in its original, unadsorbed state, these negative charges can be more stable in the potential of the Na^+ cation, and thus the electron redistribution results in enhanced molecular polarity. Therefore, in the adsorbed state, the halogen atoms are, on average, located near the Na atom, and the H atom is far from it. Furthermore, the single F NMR spectrum shows that in the motional state of the adsorbed molecule, there are two F atoms in equivalent positions regarding the potential of the Na^+ cation. Therefore, we can conclude that the Na atom comes nearly into line with C and H atoms in the adsorbed $CHClF_2$ molecule. This coordinate structure of the adsorbed molecule, which is shown in Fig. 5, is consistent with the model previously proposed on the basis of the FTIR experiment (Katoh et al., 1997).

When the adsorption amount is increased, the adsorbed molecules are destabilized by the mutual molecular collisions, and the duration of the adsorbed state is shortened. Once the molecule escapes from the potential of the Na^+ cation into surface areas other than the cation sites, or into a void space in the supercage, then the deflection of the charge distribution in the adsorbed molecule is relaxed. Thus, when the adsorption amount

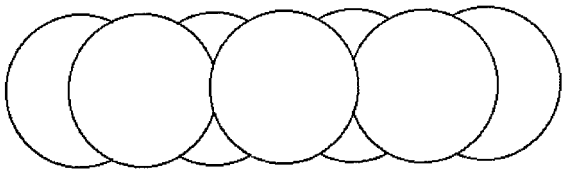

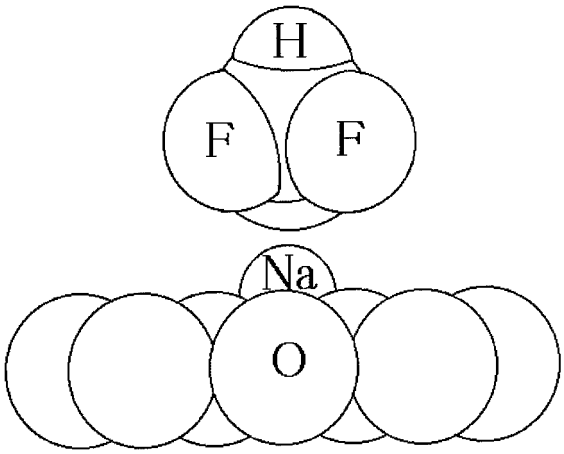

Figure 5. Adsorptive coordination model of the $CHClF_2$ molecule on the Na^+ site in the wall surface of NaY5.6 zeolite.

Table 1. Longitudinal relaxation time (T_1), signal intensity, and nuclear Overhauser enhancement (NOE) factor of the F nuclei in the $CHClF_2$ molecule under H decoupling.

Adsorption amount (molecule/cell)	T_1 (ms)		Signal intensity[a]		
	Without decoupling	Under decoupling	Without decoupling ($\times 10^2$)	Under decoupling	NOE factor
9	10.54 ± 0.37	11.73 ± 0.31	3.25	64.3	0.197
27	14.74 ± 0.24	15.07 ± 0.21	3.45	71.4	0.207
50	10.15 ± 0.09	10.13 ± 0.22	3.33	69.2	0.208

[a]Signal accumulations were done 64, 24, and 16 times for samples with adsorption amount 9, 27, and 50 molecules per unit cell, respectively.

increases, both the observed resonance frequency and the chemical shift approach those in the state free from the potential of the Na^+ cation.

3.3. Longitudinal Relaxation Time of the Adsorbed Molecule

3.3.1. Nuclear Overhauser Enhancement Factor and Temperature Dependence of Relaxation Time. In general, a nuclear spin interacts with its surroundings through the local magnetic field produced on it. Various molecular motions make this magnetic field time-dependent. When the time variation of the magnetic field contains Fourier components which correspond to the field's Larmor frequency, the magnetic interaction gives the spin an efficient relaxation process. The level of efficiency is determined by the strength of the magnetic interaction and by the length of time in which the magnetic field keeps a coherent temporal development in the molecular motion. This period is usually called the correlation time of the molecular motion (Abragam, 1961).

The principal relaxation mechanisms in the nuclear spin system in an adsorbed $CHClF_2$ molecule are the magnetic dipole-dipole interactions among the H and F nuclei, and the chemical shift anisotropy, also known as the CSA, (Engelhart and Michel, 1987); the latter mechanism is important especially for the F nuclei with non-spherical electron environments. The relevant molecular motions are rotational and translational diffusions of the $CHClF_2$ molecules in the zeolite. In this section we will first consider the relative importance to the relaxation mechanisms of the dipole-dipole interaction between H and F nuclei; next, we examine the extent of the motional activity of the adsorbed molecule, which can be estimated from the correlation time of the molecular motion.

Using three representative adsorption amounts of the sample, we measured both the steady-state signal intensities and the longitudinal relaxation times of the F nucleus under the H decoupling condition at 20°C. As Table 1 shows, there is little difference between the observed T_1 of F with or without decouplings. Furthermore, when the relaxation is assumed to occur only due to the dipole-dipole interaction between H and F nuclei, the expected maximum nuclear Overhauser enhancement (NOE) factor of ^{19}F is 0.53 (Martin et al., 1980b). However, the observed NOE factor, as is shown in Table 1, was actually approximately 0.2. These results suggest that previously mentioned dipole-dipole interaction does not have a significant effect on the relaxation of the F nuclei. This would mean that the principal relaxation mechanisms of the F nuclei are the chemical shift anisotropy and the dipole-dipole interaction between the F nuclei. On the other hand, for the relaxation of the H nucleus, the dipole-dipole interaction between H and F nuclei can be considered more effective than CSA, as in the case of $CHCl_3$ molecule (Ishiwata and Ishii, 1991; Maler and Kowalewski, 1992).

We measured the relaxation times T_1 of two samples, with the adsorption amounts, respectively, of 43 and 50 molecules per unit cell, in the temperature range of -25 to $+25$°C. Figure 6 shows the temperature dependence of T_1 for H and F nuclei. In this figure, both T_1's become shorter when the temperature decreases. Let us consider the temperature dependence of T_1 for F. When a single correlation time τ_0 is assumed for the molecular rotational motion relevant to the F relaxation, the theoretical relaxation rate due to the CSA, and the dipole-dipole interaction is given by Abragam (1961) as,

$$\frac{1}{T_1} = \frac{3}{10}\omega_0^2\delta^2\left(1+\frac{\eta^2}{3}\right)\frac{\tau_0}{1+\omega_0^2\tau_0^2} + \frac{3}{10}\frac{\gamma_F^4\hbar^2}{r_{FF}^6}\left(\frac{\tau_0}{1+\omega_0^2\tau_0^2}+\frac{4\tau_0}{1+4\omega_0^2\tau_0^2}\right), \quad (1)$$

where γ_F is the gyromagnetic ratio of F, ω_0 the larmor frequency of F, δ the CSA component in the bonding

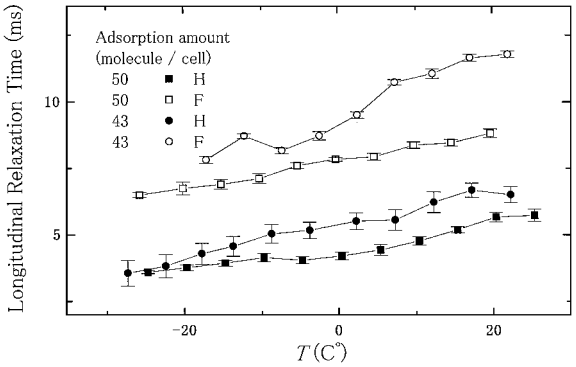

Figure 6. Temperature dependences of the longitudinal relaxation times for H and F nuclei in the $CHClF_2$ molecule adsorbed on NaY5.6 zeolite with the adsorption amounts of 43 and 50 molecules per unit cell. The curved lines are guides to the eye.

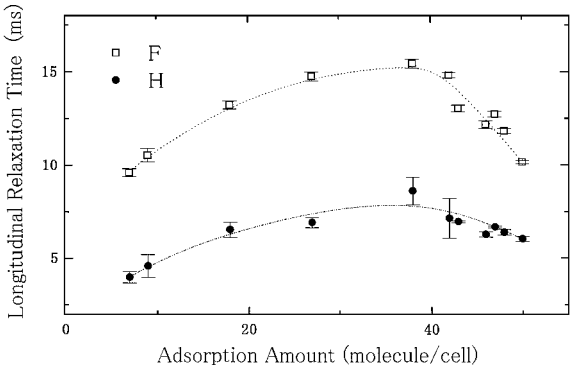

Figure 7. Adsorption amount dependences of the longitudinal relaxation times for H and F nuclei in the $CHClF_2$ molecule adsorbed on NaY5.6 zeolite at 20°C. The dotted lines are added only to guide the eye.

C-F direction of the molecule-fixed frame, η the asymmetry of the CSA components normal to the C-F axis, and r_{FF} the distance between two F atoms in the $CHClF_2$ molecule. As the function of τ_0, T_1 in Eq. (1) becomes the maximum at $\omega_0\tau_0 \cong 1$. When $\omega_0\tau_0 \gg 1$, which corresponds to a slow regime of the molecular motion, T_1 increases with τ_0. On the other hand, when $\omega_0\tau_0 \ll 1$, which corresponds to a rapid regime of the molecular motion, T_1 increases as τ_0 decreases. Molecular motions in the present case are thermal activated processes with an appropriate activation energy E_{ac}; therefore, τ_0 has a logarithmic relation to a temperature T as in the Arrhenius' equation (Slichter, 1964);

$$\tau_0 \propto \exp\left(\frac{E_{ac}}{k_B T}\right), \tag{2}$$

where k_B is the Boltzmann constant. Equation (2) means that τ_0 increases as the temperature decreases. Now in our case, the measured T_1 values decrease with the temperature. This temperature dependence of T_1 corresponds to the condition of $\omega_0\tau_0 \ll 1$ mentioned above, namely, that in which molecular motions of the adsorbed molecules are in the rapid regime. Thus, T_1 decreases with an increase in τ_0.

In the case of the H relaxation, the dipole-dipole interaction between H and F nuclei cannot be ignored. For this interaction, the τ_0 dependence of T_1 can also be illustrated by the similar relation with Eq. (1) (Martin et al., 1980c). From the experimental result of H shown in Fig. 6, the condition of the rapid molecular motion also holds for the H nucleus. Therefore, the experimental adsorption-amount dependences of T_1 can be explained by the length of the correlation time which corresponds to the motional activity of the adsorbed molecule.

3.3.2. Relation Between Relaxation Times and Adsorption Amounts. Figure 7 shows the relaxation times T_1 of H and F nuclei for various adsorption amounts. In contrast to the comparatively simple chemical shift, the dependencies of T_1 on the adsorption amount in this figure are more complex. As the adsorption amount increases, the relaxation times for both the H and F nuclei at first gradually lengthen, reaching their respective maximums; this lengthening is followed by the relatively sharp decrease in the relaxation times for the high adsorption amounts in our experiment. We will now examine the three ranges of adsorption, low, middle, and high. In the low range of the adsorption, the amount being less than 20 molecules per unit cell, the number of the $CHClF_2$ molecules adsorbed on the zeolite is lower than the number of Na^+ in the unit cell; but in the middle range of adsorption amounts, that is 30–40 molecules per unit cell, the number of adsorbed $CHClF_2$ molecules is nearly equal to the number of Na^+.

In the low range of adsorption amounts, the $CHClF_2$ molecule is tightly adsorbed at each Na^+ site, and the lifetime of the adsorbed state τ_{ad} is long. It is this strong interaction between the Na^+ cation and the adsorbed molecule which lengthens the correlation time τ_0 in the motion of the adsorbed molecule. Thus the high relaxation efficiency at the Na^+ adsorption site shortens T_1 for both nuclei. Since it is assumed that $\tau_0 \ll \tau_{ad}$, the excess magnetic energy obtained by the 180° rf pulse in the inversion recovery experiment can be fully

relaxed to a thermal bath during the adsorbed state of the $CHClF_2$ molecule. Moreover, for the $CHClF_2$ molecule, the Na^+ site is the most efficient relaxation sink in the entire zeolite structure.

In the middle range of adsorption amounts, the physically adsorbed molecules interact and collide with each other. Consequently, the molecules move non-locally around various adsorption sites, and some of them jump into the void space. Because of these rapid, random molecular motions, the adsorption lifetime τ_{ad} and the correlation time τ_0 of the molecular motion are both shortened, and the relaxation time T_1 is lengthened as compared with those times in the low range of adsorption amounts.

In the high range of adsorption amounts many molecules are found in the void space. As the number of the molecules in the void space increases, the mobility of the molecules decreases because of the intermolecular interaction; accordingly, the relaxation times T_1 for both the shorten with the increasing the adsorption amount.

As Fig. 7 clearly illustrates, the T_1 of F is longer than that of H, regardless of the molecule's adsorption amount. This difference can be explained by the motional activity between the F and H atoms in the $CHClF_2$ molecule, whether in the molecule adsorbed on Na^+ or in the void space of zeolite. In the adsorptive coordination model mentioned above, two F and one Cl atoms in the $CHClF_2$ molecule are located near to the Na^+ on the cage wall. Since, in the present case, these atoms are not chemically bound to the Na^+, the F and Cl atoms can rotate around the C-H bonding axis. This rapid pivoting motion randomly modulates both the chemical shift anisotropy of the F nuclei and the dipole-dipole interaction between the two F nuclei. The F relaxation therfore becomes less efficient, due to the relatively short correlation time of the fast pivoting motion.

However, this pivoting motion cannot have much influence on the motion of the H atom, as the H atom is on the pivoting axis. It is the rotational tumbling of the C-H axis itself which has the more important role in the H relaxation. It is well known that for a symmetrical molecule, such as chloroform in an isotropic liquid, or in anisotropic liquid crystals (Courtieu et al., 1977; Vold et al., 1978), the pivoting motion around the C-H bonding axis is much faster than the tumbling of the C-H axis itself. Similarly, in the present adsorption on the zeolite, the relatively slow tumbling shortens the H relaxation time T_1 when compared with that of the F nucleus. This is the reason that the T_1 of F is longer than that of H at every adsorption amount.

Figure 7 also shows that T_1 difference between F and H in the high adsorption range is less than in the low and middle ranges. Because of the mutual molecular collisions in the high adsorption range, the adsorption lifetime τ_{ad} is short when compared with those the in other two ranges. In addition, in the high adsorption range the $CHClF_2$ molecule spends a fairly long time in the cavity void. Since the void space is substantially free from the attractive potential of the Na^+ cation, the difference in the correlation times between the pivoting and tumbling motions is less there than it is when the molecule is adsorbed on the Na^+ cation which restricts the tumbling motion. Therefore, in the high range of adsorption amounts, the T_1 of H approaches that of F as the adsorption amount increases.

3.4. Simulation of the Adsorption Isotherms

Let us now look closely at the isotherms of the $CHClF_2$ molecule shown in Fig. 1. As a function of the equilibrium pressure of the $CHClF_2$ gas at each temperature, the adsorption amount is at first proportional to the pressure in the Henry's law region, but then the adsorption amount shows a slight saturation, followed again by a linear increase with the increasing pressure, which is slower than that in the Henry's law region. We obtained the same results in Xe adsorption as well (Yoshida et al., 1988 and 1989). The result obtained here is similar to those of the Xe adsorption observed by Aristov et al. (1967). From their results, they considered that localized and nonlocalized Xe adsorptions often coexist on the zeolites such as LiX and NaX. These features of the isotherms can also be interpreted by a superimposed two-site Langmuir model (Koresh and Soffer, 1983).

Our present data are highly reproducible. No hystereses have been observed in the isotherms; that is, the adsorbed amount in the adsorptive process is exactly equal to that in the desorptive one at the same equilibrium pressure. From these facts, it becomes evident that the $CHClF_2$ adsorption occurs in the intense potential field of the Na^+ cation, and is not due simply to a pore filling (Hara and Takahashi, 1975). Thus, we must consider whether the $CHClF_2$ adsorption occurs on localized or nonlocalized sites in NaY5.6 zeolite. In order to understand the features of the isotherms in Fig. 1, therefore, we examined Kiselev's equation

(Kiselev, 1958; Aristov et al., 1967) and Hill's equation using curve-fitting of the adsorption isotherms, as we had previously done in our analysis of the Xe adsorption data (Yoshida et al., 1988, 1989).

Kiselev's and Hill's equations are given as

$$P = \frac{\theta}{K_1'(1-\theta)(1+K_2'\theta)}, \tag{3}$$

and

$$P = \frac{\theta}{K_1(1-\theta)} \exp\left(\frac{\theta}{1-\theta} - K_2\theta\right), \tag{4}$$

respectively, where P is the equilibrium pressure, θ the surface coverage, K_1', K_1 the equilibrium constants of adsorbate-adsorbent (Henry constant), and K_2', K_2 those of adsorbate-adsorbate. In Eqs. (3) and (4), the coverage θ is given by a volume ratio V/V_m, where V is a $CHClF_2$ gas volume under normal conditions (0°C, 1 atm) corresponding to an adsorption amount at the equilibrium pressure, and V_m is its saturated value at a constant experimental temperature. The result of simulations is shown in Table 2 for three isotherms observed at 0, 10 and 20°C. At all the temperatures, the sum of the squared residuals in the adsorption data for the Hill's equation is smaller than that for the Kiselev's one. Furthermore, although it is difficult to decide reasonable magnitudes for the values for the constants K_1', K_1, K_2' and K_2 from the chemical viewpoint, the negative values of K_2' at 10 and 20°C in the Kiselev's equation are not meaningful. Therefore, we should select Hill's equation for reproducing the experimental isotherms.

Hill's equation is reduced to Langmuir's equation describing typical localized adsorption when the adsorption amount is extremely small, while kiselev's equation corresponds only to localized adsorption. Since Hill's equation holds over a wide range of the adsorption amounts, its meaning changes from localized adsorption to non-localized as the adsorption amount increases. Thus, the conclusions obtained from the analysis of the isotherms is not inconsistent with the results of the NMR experiment.

4. Conclusion

From the H and F NMR data on the chemical shifts, from the relaxation times for the $CHClF_2$ molecule at relatively low adsorption amounts, and from the simulation of the adsorption isotherms, it is possible to conclude that the F atoms of the adsorbed $CHClF_2$ molecule are closer to the Na^+ cation, while the H atom is far from it; and that the Na^+ cation site is the most efficient relaxation sink in the entire zeolite structure and its intense potential field enhances anisotropy in the moleculer motion of the adsorbed $CHClF_2$. This adsorptive coordination model is consistent with the one previously proposed on the basis of the FTIR data (Katoh et al., 1997). Moreover, the experimental adsorption isotherms for the adsorption amounts up to 50 molecules per unit cell can be well reproduced by Hill's equation.

Table 2. Adsorption parameters of the $CHClF_2$ molecule on NaY5.6 zeolite fitted to Kiselev's and Hill's equations.

Temperature (°C)	K_1'[a] ($Torr^{-1}$)	K_2' ($\times 10^{-3}$)	V_m[b] (mol./cell)	SS[c]	Data point
Kiselev's equation					
0	7.534	8.57	51.78	0.490	20
10	6.469	−1.678	50.42	1.233	34
20	6.725	−6.220	50.98	0.250	29
Temperature (°C)	K_1[a] ($Torr^{-1}$)	K_2	V_m[b] (mol./cell)	SS[c]	Data point
Hill's equation					
0	9.936	2.163	62.88	0.250	20
10	6.469	1.667	63.79	1.070	34
20	6.725	2.223	63.79	0.142	29

[a]Parameters K_1', K_2', K_1, and K_2 are defined in Eqs. (3) and (4) in the text for Kiselev's and Hill's equations, respectively.
[b]V_m is given by a coverage $\theta = V/V_m \cdot \theta$ is defined in the text.
[c]Sum of the squared residuals in fitting the adsorption data.

Nomenclature

μ	Dipole moment
ΔH	Enthalpy change on adsorption
T_1	Longitudinal relaxation time
γ_F	Gyromagnetic ratio
h	Planck constant
ω_0	Larmor frequency
τ_0	Correlation time of molecular motion
r_{FF}	Interatomic distance of two fluorines in $CHClF_2$
E_{ac}	Activation energy
k_B	Boltzmann constant
T	Temperature
τ_{ad}	Adsorption lifetime
P	Equilibrium pressure
K_1	Adsorption constant
K_2	Dimensionless adsorption constant
θ	Coverage
V_m	Maximum adsorption amount
δ	Chemical shift anisotropy
η	Asymmetry of CSA

References

Abragam, A., *Principles of Nuclear Magnetism*, Ch. 8, Clarendon, Oxford, 1961.

Aristov, B.G., V. Bosacek, and A.V. Kiselev, "Dependence of Adsorption of the Krypton and Xenon by Crystals of Zeolite Lix and NaX on Pressure and Temperature," *Trans. Faraday Soc.*, **63**, 2057–2067 (1967).

Beeson, E.L., T.L. Weatherly, and Q. Williams, "Molecular Constants of Chlorodifluoromethane from Microwave Spectrum Analysis," *J. Chem. Phys.*, **37**, 2926–2929 (1962).

Courtieu, J.M., C.L. Mayne, and D.M. Grant, "Nuclear Relaxation in Coupled Spin Systems Dissolved in a Nematic Phase—The AX and A_2 Spin Systems," *J. Chem. Phys.*, **66**, 2669–2677 (1977).

Engelhardt, G. and D. Michel, *High-Resolution Solid-State NMR of Silicates and Zeolites*, Ch. 1, John Wiley & Sons, Chichester, 1987.

Hara, N. and H. Takahashi, *Zeolite—The Bases and Applications* [Japanese], p. 62, Kodansha Scientific, Tokyo, 1975.

Hill, T.L., "Statistical Mechanics of Multimolecular Adsorption II. Localized and Mobile Adsorption and Absorption," *J. Chem. Phys.*, **14**, 441–453 (1946).

Hill, T.L., "Statistical Mechanics of Multimolecular Adsorption III. Introductory Treatment of Horizontal Interactions, Condensation and Hysteresis," *J. Chem. Phys.*, **15**, 767–777 (1947).

Ishiwata, M. and Y. Ishii, "^{13}C and ^{1}H NMR Relaxation of Chloroform Dissolved in a Nematic Liquid Crystal II, Dynamical Behavior of the Small Probe Molecule," *J. Phys. Soc. Jpn.*, **60**, 1743–1754 (1991).

June, R.L., A.T. Bell, and Theodorou D.T., "Molecular Dynamics Study of Methane and Xenon in Silicalite," *J. Phys. Chem.*, **94**, 8232–8240 (1990).

Katoh, M., H. Hatayama, T. Yamasaki, and S. Ozawa, "Adsorption of $CHClF_2$ onto Ion-Exchanged ZSM-5 Zeolites," *Nippon Kagaku Kaishi* [Japanese], (**1997**), 24–32.

Kiselev, A.V., "Adsorbate-Adsorbate Interaction in the Adsorption of Vapors on Graphitized Carbon Blacks," *Kolloidn Zh.*, **20**, 320–331 (1958).

Koresh, J. and A. Soffer, "Application of the Two-site Langmuir Isotherm to Microporous Adsorbents," *J. Colloid Interface Sci.*, **92**, 517–524 (1983).

Liu, S.B., L.J. Ma, M.W. Lin, J.F. Wu, and T.L. Chen, "NMR Investigation of the Distribution of Benzene in NaX and NaY Zeolites: Influence of Cation Location and Adsorbate Concentration," *J. Phys. Chem.*, **96**, 8120–8125 (1992).

Maler, L. and J. Kowalewski, "Cross-Correlation Effects in the Longitudinal Relaxation of Heteronuclear Spin Systems," *Chem. Phys. Lett.*, **192**, 595–600 (1992).

Martin, M.L., G.J. Martin, and J.J. Delpuech, *Practical NMR Spectroscopy*, Ch. 7, Heyden, London, 1980a.

Martin, M.L., G.J. Martin, and J.J. Delpuech, *Practical NMR Spectroscopy*, p. 23, Heyden, London, 1980b.

Martin, M.L., G.J. Martin, and J.J. Delpuech, *Practical NMR Spectroscopy*, p. 17, Heyden, London, 1980c.

Mortier, W.J., E. Van den Bossche, and J.B. Uytterhoeven, "Influence of the Temperature and Water Adsorption on the Cation Location in Na-Y Zeolites," *Zeolites*, **4**, 41–44 (1984).

O'Malley, P.J., "Formation of Benzene Clusters in Y-Type Zeolites: An Infrared Study," *Chem. Phys. Lett.*, **166**, 340–342 (1990).

Pearson, J.G., B.F. Chmelka, D.N. Shykind, and A. Pines, "Multiple-Quantum NMR Study of the Distribution of Benzene in NaY Zeolite," *J. Phys. Chem.*, **96**, 8517–8522 (1992).

Pople, J.A., W.G. Schneider, and H.J. Berstein, *High-Resolution Nuclear Magnetic Resonance*, Ch. 7, McGraw-Hill, New York, 1959.

Sherry, H.S., "The Ion-Exchange Properties of Zeolites. IV. Alkaline Earth Ion Exchange in the Synthetic Zeolites Linde X and Y," *J. Phys. Chem.*, **72**, 4086–4094 (1968).

Slichter, C.P., *Principles of Magnetic Resonance*, p. 156, Harper & Row, New York, 1964.

Talu, O., S.Y. Zhang, and D.T. Hayhurst, "Effect of Cations on Methane Adsortion by NaY, MgY, CaY, SrY, and BaY Zeolites," *J. Phys. Chem.*, **97**, 12894–12898 (1993).

Van Dun, J.J. and W.J. Mortier, "Temperature-Dependent Cation Distribution in Zeolites 1. A Statical Thermodynamical Model," *J. Phys. Chem.*, **92**, 6740–6746 (1988).

Vold, R.R., P.H. Kobrin, and R.L. Vold, "Frequency Dependent Nuclear Relaxation of Chloroform in Isotropic MBBA," *J. Chem. Phys.*, **69**, 3430–3431 (1978).

Wylie, D.J., R.P. Cooney, J.M. Seakins, and G.J. Millar, "Spectroscopic Studies of the Adsorption and Reactions of Chlorofluorocarbons (CFC-11 and CFC-12) and Hydrochlorofluorocarbon (HCFC-22) on Oxide Surfaces," *Vibrational Spectroscopy*, **9**, 245–256 (1995).

Yashonath, S., P. Demontis, and M.L. Klein, "Temperature and Concentration Dependence of Adsorption Properties of Methane in NaY: A Molecular Dynamics Study," *J. Phys. Chem.*, **95**, 5881–5889 (1991).

Yoshida, T., J. Koizumi, and Y. Akai, "Adsorption of Xenon in the Zeolitic Pore in the Henry's Law Region of the Isotherms," *Bull. Chem. Soc. Jpn.*, **61**, 989–990 (1988).

Yoshida, T., J. Koizumi and Y. Akai, "Adsorptive Behavior of Xenon in Zeolitic Pore of Faujasite," *Nippon Kagaku Kaishi* [Japanese], (**1989**), 458–462.